

Robust reactivity, neutron source, and precursor estimators for nuclear reactors



Günyaz Ablay*

Electrical and Electronics Engineering, Abdullah Gül University, 38039 Kayseri, Turkey

HIGHLIGHTS

- Robust nonlinear estimators provide accurate and online real-time calculations.
- Precursor estimator will remove performance degradation during operation.
- Accurate reactivity estimation will increase control flexibility and safety.

ARTICLE INFO

Article history:

Received 10 May 2013

Received in revised form 30 July 2013

Accepted 31 July 2013

ABSTRACT

Reactivity, precursor concentration, and external neutron source strength determine control, operation and performance of nuclear reactors. These main reactor quantities are not directly measurable and must be calculated or estimated using reactor kinetics. This study presents efficient and robust nonlinear estimation algorithms for predicting these fundamental reactor quantities. The effectiveness of the proposed estimators is assessed through chirp and step test signals in the presence of parameter uncertainties and measurement noise.

© 2013 Elsevier B.V. All rights reserved.

1. Introduction

Nuclear data acquisition and process information system developments are crucial for control and operation of nuclear reactor dynamics. Nuclear reactor dynamics are usually expressed with reactor kinetics equations. The reactor kinetics models are commonly used in many practical situations including fast transient analysis (e.g. reactor accidents) and short-term operating transient analysis (e.g. power-level reactivity effects). They are constructed with reactivity, neutron generation time, delayed neutrons, and external neutron source, which are common to all types of fission reactors (Hetrick, 1993). It is well-known that reactivity measurement is important for monitoring the reactor condition, quantification of the worth of fuel bundles, and controlling the reactor. The delayed neutrons contribute less than 1% of the neutron reproduction in fission reactors, but they are extremely important for the controllability of nuclear reactors. The external neutron source is necessary for reactor startup and for maintaining criticality in source-driven subcritical systems. One challenge is that reactivity, external neutron source, and delayed neutron

concentrations are not directly measurable quantities and must be calculated or estimated through reactor kinetics.

Estimation methods play an important role in nuclear industry since there are many quantities, e.g. reactivity, which cannot be ascertained directly by an ordinary sensor process. Two different classes of estimators are used: open-loop state estimators and dynamic estimators. Unlike the open-loop estimators, the dynamic estimators respond to a given state measurement and adjust estimates of other states to drive the predicted measured state to the actual state. Dynamic estimators use mathematical models and feedbacks from measurable states, and thus, they provide the best estimates (Martin and Edwards, 2000). The application areas of the estimators include estimation of state variables and parameters for data reconciliation (Albuquerque and Biegler, 1996; Grauf et al., 2000; Martin and Edwards, 2000), for online condition monitoring (Ablay and Aldemir, 2013; Hashemian and Feltus, 2006; Hines and Davis, 2005; Humberstone et al., 2011; Li and Bernard, 2002; Rasmussen et al., 2002; Zavaljevski et al., 2004), for critical parameter estimation (Ablay and Aldemir, 2011; Cadini and Zio, 2007; Marseguerra et al., 2003; Perez-Cruz and Poznyak, 2007; Kaiser et al., 2009; Wang et al., 2001), and for use in automatic control design (Dong et al., 2009; Na and No, 1992; Park and Cho, 1992; Reddy et al., 2008). The accuracy of estimated quantities in these practical applications usually depends on the accuracy of the mathematical models of systems. Therefore, estimators must be robust

* Tel.: +90 352 224 8800; fax: +90 352 338 8828.

E-mail address: [gunyaz.ablay@agu.edu.tr](mailto:gunnyaz.ablay@agu.edu.tr)

in the presence of disturbances, modeling and parameter uncertainties. Moreover, simple and flexible design characteristics are the other significant properties that an estimator must have in practical point of view.

The aim of this study is to provide simple, efficient and robust dynamic-estimation algorithms for reliable reactivity, external neutron source, and precursor estimations in nuclear reactors. Proposed estimation approaches are based on mathematical models of nuclear reactors and nonlinear estimation theory. The provided estimators are simple, but robust in the existence of disturbance or parameter uncertainty. These estimation approaches can be significant for online condition monitoring, data reconciliation and nuclear reactor control.

The paper is organized as follows: Section 2 describes the characterization and modeling of nuclear reactors. Section 3 provides estimation algorithms for reactivity, external source and precursor estimations. The implementation results and conclusion of the study are given in Sections 4 and 5, respectively.

2. Problem formulation and preliminaries

In the following subsections, dynamical information about nuclear reactor models and integral filters that will be used to construct state estimators is provided.

2.1. Reactor model

The prediction of time behavior of the neutron population in a nuclear reactor core is important for transient analysis and accident consequences analyses of fission reactor. The point reactor kinetics (PRK) equations are a one-speed diffusion model and a very powerful tool for describing time behavior of a nuclear reactor (Hetrick, 1993; Nahla, 2010; Sathiyasheela, 2010; Theler and Bonetto, 2010). The time-dependent and nonlinear PRK equations are given by:

$$\begin{aligned} \frac{dN(t)}{dt} &= \frac{\rho(t) - \beta}{\Lambda} N(t) + \sum_{i=1}^6 \lambda_i C_i(t) + S(t) \\ \frac{dC_i(t)}{dt} &= \frac{\beta_i}{\Lambda} N(t) - \lambda_i C_i(t), \quad i = 1, \dots, 6 \end{aligned} \quad (1)$$

where N (in watts) is the neutron power, C_i (in watts) represents the precursor concentration for i th delayed neutron precursor, ρ (in $\Delta k/k$) is the net reactivity, S (in watts per second) is an effective neutron source strength provided by external sources, λ_i (in 1/s) is the decay constant for i th delayed neutron precursor, β_i is the fractional yield of i th precursor group, β is the total precursor yield fraction $\beta = \beta_1 + \dots + \beta_6$, and Λ (in s) is the mean neutron generation time which is about 10^{-8} s for fast reactors and about 10^{-3} s for thermal reactors. The net reactivity ρ (in $\Delta k/k$) depends on the size of reactor, amounts and densities of various materials, and neutron cross sections. Since all these parameters are affected by temperature, pressure and fission fragments, reactivity depends on the power history of a reactor. Thus, net reactivity of nuclear reactors is summation of the external reactivity input and reactivity feedback which is a function of neutron power, in general. Namely,

$$\rho(t) = \rho_c(t) - \alpha N(t) \quad (2)$$

where ρ_c is the external reactivity input and α is the reactivity feedback coefficient.

For simplification, we can also consider the case in which all delayed neutrons are represented by one effective delayed group by defining an averaged decay constant as

$$\frac{1}{\lambda} = \frac{1}{\beta} \sum_{i=1}^6 \frac{\beta_i}{\lambda_i} \quad (3)$$

Then, the PRK can be simplified as

$$\begin{aligned} \frac{dN(t)}{dt} &= \frac{\rho(t) - \beta}{\Lambda} N(t) + \lambda C(t) + S(t) \\ \frac{dC(t)}{dt} &= \frac{\beta}{\Lambda} N(t) - \lambda C(t) \end{aligned} \quad (4)$$

where λ is the averaged decay constant and C represents the effective precursor concentration. It is often convenient to use simplified PRK (4) while it becomes useless for very small reactivities.

It is possible to reduce the set of coupled differential equations (1) to a single integro-differential equation in terms of N . For this aim, a solution to nonhomogenous precursor concentration equations can be obtained as

$$C_i(t) = C_{i,0} e^{-\lambda_i t} + \frac{\beta_i}{\Lambda} e^{-\lambda_i t} \int_0^t e^{\lambda_i \tau} N(\tau) d\tau \quad (5)$$

where initial conditions $C_{i,0}$ are equal to

$$C_{i,0} = \frac{\beta_i}{\lambda_i \Lambda} N_0 \quad (6)$$

Substituting (6) into (5), the solution of precursor equations is as follows:

$$C_i(t) = \frac{\beta_i}{\Lambda} e^{-\lambda_i t} \left[\frac{N_0}{\lambda_i} + \int_0^t e^{\lambda_i \tau} N(\tau) d\tau \right] \quad (7)$$

Substituting (7) into the neutron power Eq. (1), a nonlinear integro-differential form of the PRK can be obtained as:

$$\begin{aligned} \frac{dN(t)}{dt} &= \frac{\rho(t) - \beta}{\Lambda} N(t) + \Phi(t) + S(t) \\ \Phi(t) &= \frac{1}{\Lambda} \sum_{i=1}^6 \beta_i e^{-\lambda_i t} \left[N_0 + \lambda_i \int_0^t e^{\lambda_i \tau} N(\tau) d\tau \right] \end{aligned} \quad (8)$$

where Φ is the integral equation. For one effective delayed group representation (4), Eq. (8) can be rewritten as:

$$\begin{aligned} \frac{dN(t)}{dt} &= \frac{\rho(t) - \beta}{\Lambda} N(t) + \Phi(t) + S(t) \\ \Phi(t) &= \frac{\beta}{\Lambda} e^{-\lambda t} \left[N_0 + \lambda \int_0^t e^{\lambda \tau} N(\tau) d\tau \right] \end{aligned} \quad (9)$$

where λ is defined in Eq. (3). The nonlinear integro-differential equations given in (8) and (9) will be used for reactivity and external source estimations for nuclear reactors, respectively.

2.2. Integral Filters

Integral filters are commonly used in practical control applications to filter out the effects of noise in measurements and to calculate derivative of references or measurements. Mathematically, these filters can be composed of n th order differential equations, but the first and second order filters are usually used in control systems. A first order low pass filter is constructed as

$$\tau \frac{dz(t)}{dt} = -z(t) + g(t) \quad (10)$$

where z is a small enough positive time constant and g is a noisy signal which may or may not be differentiable. It is obvious that if τ is sufficiently small, the output of low-pass filter is

$$z(t) \approx g(t) \quad (11)$$

This means that the low-pass filter eliminates the high frequency component (or noisy part) of signal g , but preserves slow-varying component of function g .

Now, consider a second order low-pass filter defined by the following equation (Lu and Hedrick, 2000):

$$\frac{\tau^2}{2} \frac{d^2 z(t)}{dt^2} = -\tau \frac{dz(t)}{dt} - z(t) + g(t) \quad (12)$$

Such a filter exists because its roots always have negative real parts for $\tau > 0$, i.e. $s_{1,2} = (-1 \pm i)$. Again, if τ is sufficiently small, the output of low-pass filter approaches the slow-varying component of signal, i.e. $z(t) \approx g(t)$. The second order low-pass filter eliminates the high frequency component (or noise) of the signal g with a higher precision compared to the first order low-pass filter.

Similarly, higher-order low-pass filters can be constructed. The advantage of higher-order low-pass filters are the stronger noise rejection and higher precision by comparison to low order low-pass filters. However, the computational burden and time delay in the signals increase with the order of filters.

3. State and parameter estimations using the reactor model

Simple precursor concentration, source term and reactivity estimation algorithms for nuclear reactors are provided below. It should be noted that in the following algorithms, the second order filter can be used for more accurate estimations while the first order filter is designed for simplicity. Furthermore, the time dependency of the error functions will not be shown in notations for simplicity. In estimators, since a constant gain δ appears only in the estimation algorithms, it can be selected arbitrarily large.

3.1. Reactivity estimation

The reactivity is the control input of nuclear reactors. As described in Section 2, the reactivity consists of intrinsic feedback reactivity and external reactivity input which is provided by shim control mechanisms for controlling reactor power. Computation of reactivity feedback is one of the central problems of nuclear reactors. The reactivity measurements are obtained through the reactor kinetics and counting methods in critical reactors (Ansari, 1991; Cacuci, 2010; Gallmeier and Steichele, 1994; Hu et al., 2013; Perez-Cruz and Poznyak, 2007; Rácz, 1992; Wright, 2005). Since the external neutron source term can be ignored in high-power reactors, a simple reactivity estimation algorithm can be obtained by using neutron power dynamics (8) as:

$$\begin{aligned} \frac{d\hat{N}(t)}{dt} &= \frac{\psi(t)}{\Lambda} \hat{N}(t) - \frac{\beta}{\Lambda} \hat{N}(t) + \Phi(t) \\ \psi(t) &= \delta_r \text{sign}(N(t)e_N) \end{aligned} \quad (13)$$

where \hat{N} is the estimation of N , the integral equation Φ is defined in Eq. (8), δ_r is a constant estimator gain, and the error state is defined by $e_N = N - \hat{N}$. The $\text{sign}(\cdot)$ function is the unit vector defined by:

$$\text{sign}(e) = \frac{e}{|e|} \quad (14)$$

The time derivative of power error state (from (8) to (13)) is obtained as:

$$\frac{de_N}{dt} = \frac{\rho(t) - \psi(t)}{\Lambda} N(t) \quad (15)$$

where $N(t)$ is measurable. Convergence of error dynamics can be determined by the Lyapunov theorem (Khalil, 2002) which states that for a Lyapunov function defined by a positive definite, quadratic and scalar function of state variables, its derivative must be negative for stability. This approach obviates the need to solve the differential equations when evaluating their convergence (or stability) properties. Since there are no generally applicable rules for defining Lyapunov functions, trial/error and mathematical/physical insight are often used. To analyze convergence of the

error dynamics (15), a Lyapunov function is defined as $L = e_N^2/2$, and then we have

$$e_N \frac{de_N}{dt} = \frac{\rho(t) - \psi(t)}{\Lambda} Ne_N \leq \frac{1}{\Lambda} (|\rho(t)| - \delta_r) |Ne_N| \quad (16)$$

If the estimator gain δ_r is selected large enough to satisfy $\delta_r > |\rho(t)|$, it will be $e_N \dot{e}_N < 0$ such that the power error converges to zero, $e_N \rightarrow 0$. To extract the reactivity, we need to use a low-pass filter as defined in Section 2.2. After the power error reaches zero, the reactivity is equal to the low-pass filtered value of the discontinuous function $\delta_r \text{sign}(Ne_N)$, i.e. for a first order filter,

$$\begin{aligned} \tau \frac{dz(t)}{dt} &= -z(t) + \delta_r \text{sign}(Ne_N) \\ \rho(t) &= z(t) \end{aligned} \quad (17)$$

where the reactivity $\rho(t)$ is extracted from $z(t)$ after $e_N \rightarrow 0$.

3.2. External neutron source estimation

The external neutron source is necessary for reactor startup and an important power source for low-power nuclear reactors, e.g. space reactors (Shtessel, 1998; Upadhyaya et al., 2005). The effect of external source changes in time due to decay process (Neeb, 1997), and external source contributes to tritium level in coolant (Shaver and Lanning, 2010). Hence, external source estimation may be useful for tracking its level in low-power reactors and tritium level traction in the coolant for high-power reactors. A simple external neutron source estimation algorithm can be obtained from neutron power dynamics when the reactivity is known. This assumption is specifically valid for source-driven subcritical systems since reactivity can be measured by Feynman-alpha (Pázsit et al., 2004), Rossi-alpha (Muñoz-Cobo et al., 2011), Cf-252 (Mihalczko et al., 1990), and source modulation (Wright, 2005) methods. Consider a power estimation algorithm

$$\frac{d\hat{N}(t)}{dt} = \frac{\rho(t) - \beta}{\Lambda} \hat{N}(t) + \Phi(t) + \delta_s \text{sign}(e_N) \quad (18)$$

where N is measurable, ρ is assumed to be known, Φ is the integral equation given in (9), and δ_s is a constant estimator gain. It should be noted that since external source has very small variations (nearly constant), use of one effective delayed group representation (9) provides good estimation results and simplicity. From Eqs. (9) and (18), the dynamic of power estimation error $e_N = N - \hat{N}$ is governed by

$$\frac{de_N}{dt} = \frac{\rho - \beta}{\Lambda} e_N + S - \delta_s \text{sign}(e_N) \quad (19)$$

Similar to Section 3.1, for a Lyapunov function $L = e_N^2/2$, we have

$$e_N \frac{de_N}{dt} = \frac{\rho - \beta}{\Lambda} e_N^2 + Se_N - \delta_s |e_N| \leq \left(\left| \frac{\rho - \beta}{\Lambda} \right| |e_N| + |S| - \delta_s \right) |e_N| \quad (20)$$

Here, if the estimator gain δ_s is selected large enough to satisfy $\delta_s > \left| \frac{\rho - \beta}{\Lambda} \right| |e_N| + |S|$, it will be $e_N \dot{e}_N < 0$ such that the power error converges to zero, $e_N = 0$. To obtain the source term, we need to use an integral (low-pass) filter as defined in Section 2.2. Once the error reaches zero, the source term is equal to the low-pass filtered value of the discontinuous function $\delta_s \text{sign}(e_N)$, i.e. for a first order filter,

$$\begin{aligned} \tau \frac{dz(t)}{dt} &= -z(t) + \delta_s \text{sign}(e_N) \\ S(t) &= z(t) \end{aligned} \quad (21)$$

where $z(t)$ is equal to the source term $S(t)$ after $e_N \rightarrow 0$.

3.3. Precursor concentration estimation

The one delayed group PRK model has a measurable state variable, neutron power, and an unmeasurable state variable, precursor concentration. Therefore, the precursor estimation is a classical state estimation problem that can be solved with a state estimator design. Assume that nuclear reactor is at high power so that the extraneous neutron source is negligible. A simple and efficient estimation algorithm for precursor concentration as described in [Ablay and Aldemir \(2011\)](#) by using six-group precursor Eq. (1) is given by:

$$\begin{aligned} \frac{d\hat{N}(t)}{dt} &= \frac{\rho(t) - \beta}{\Lambda} \hat{N}(t) + \sum_{i=1}^6 \lambda_i \hat{C}_i(t) + \delta_c \text{sign}(N(t) - \hat{N}(t)) \\ \frac{d\hat{C}_i(t)}{dt} &= \frac{\beta_i}{\Lambda} \hat{N}(t) - \lambda_i \hat{C}_i(t) \end{aligned} \quad (22)$$

where (\hat{N}, \hat{C}_i) are estimations of (N, C_i) and δ_c is a constant estimator gain. The estimation errors for neutron power and precursor concentration are defined as $e_N = N - \hat{N}$ and $e_{C,i} = C_i - \hat{C}_i$, respectively. From Eqs. (1) and (22), the dynamic of power estimation error state is

$$\frac{de_N}{dt} = \frac{\rho - \beta}{\Lambda} e_N + \sum_{i=1}^6 \lambda_i e_{C,i} - \delta_c \text{sign}(e_N) \quad (23)$$

Similar to previous sections, a Lyapunov function can be selected as $L = e_N^2/2$, then its derivative is

$$\begin{aligned} e_N \frac{de_N}{dt} &= \frac{\rho - \beta}{\Lambda} e_N^2 + e_N \sum_{i=1}^6 \lambda_i e_{C,i} - \delta_c |e_N| \\ &\leq \left(\left| \frac{\rho - \beta}{\Lambda} \right| |e_N| + \left| \sum_{i=1}^6 \lambda_i e_{C,i} \right| - \delta_c \right) |e_N| \end{aligned} \quad (24)$$

Here, the observer gain δ_c is selected large enough to satisfy $\delta_c > |(\rho - \beta)/\Lambda| |e_N| + \left| \sum_{i=1}^6 \lambda_i e_{C,i} \right|$. Hence, the derivative of the Lyapunov function turns out to be negative definite, $e_N \dot{e}_N < 0$, which indicates error convergence to zero. For the precursor concentration, we have the following error dynamics,

$$\frac{de_{C,i}}{dt} = \frac{\beta_i}{\Lambda} e_N - \lambda_i e_{C,i} \quad (25)$$

After $e_N \rightarrow 0$ with increasing time due to large gain δ_c , the error state $e_{C,i}$ will have an exponentially decaying solution, $e_{C,i} = e_{C,i}(0) \exp(-\lambda_i t)$ for the initial conditions $e_{C,i}(0)$. Hence, the estimation error on the precursor concentration decays to zero, i.e. $e_{C,i} \rightarrow 0$ in some time (around $4/\lambda_i$ s since λ_i 's are the time constants for precursor error dynamics).

4. Numerical results

The implementation of the estimation approaches is performed with MATLAB/Simulink programs. The numerical solution method is the MATLAB's ODE15s (a variable order solver based on the numerical differentiation formulas for stiff problems ([Shampine and Reichelt, 1997](#))) with relative accuracy tolerance of 10^{-9} , since the MATLAB's numerical solution methods (ODEs) provide the best results for PRK solutions according to [Aboanber \(2006\)](#). It is assumed that the neutron power measurement is exposed to normally distributed measurement noise with zero mean and a standard deviation of 0.013 (or around $\pm 5\%$ of the normalized power value). By considering contemporary digital technologies,

Table 1
U-235 neutron data for PRK model.

Group	Decay constant, λ_i (1/s)	β_i/β	Delayed fraction, β_i
1	0.0126	0.0323	2.10×10^{-4}
2	0.0301	0.218	1.42×10^{-3}
3	0.1118	0.195	1.27×10^{-3}
4	0.3014	0.397	2.58×10^{-3}
5	1.1363	0.115	7.50×10^{-4}
6	3.0137	0.0415	2.70×10^{-4}
Total delayed neutron fraction, β			0.0065
Mean neutron generation time, Λ (s)			3×10^{-5}
Averaged decay constant, λ (1/s)			0.0769
Reactivity feedback coefficient, α			0.003

it is convenient to use very high sampling frequency (above GHz or below nanoseconds level) where digital signals are nearly continuous, so discretization is not needed for the proposed approaches. In the estimations, the second-order low pass filter given in Eq. (12) with $\tau = 0.05$ is used. The PRK model parameters used in simulations are given in [Table 1](#).

In numerical simulations, the $\text{sign}(\cdot)$ function (or unit vector) in the estimators are replaced with saturation function (Eq. (26)) to ease numerical calculations by providing a continuous approximation to the $\text{sign}(\cdot)$ function.

$$\text{sat}\left(\frac{e}{\varepsilon}\right) = \begin{cases} e/|e|, & \text{if } |e/\varepsilon| > 1 \\ e/\varepsilon, & \text{if } |e/\varepsilon| \leq 1 \end{cases} \quad (26)$$

where ε is known as boundary layer width and is a small constant, e.g. $\varepsilon = 0.01$ in the following applications.

The step and chirp signals are used for test input reactivity signals in simulations. Chirp signal is commonly used for system identification or for testing the performance of a system ([You et al., 2012](#)). The chirp signal is a sine wave whose frequency increases at a linear rate with time, and is given by

$$\omega(t) = A \sin(2\pi(f_0 + \mu t)t) \quad (27)$$

where amplitude A , starting frequency f_0 and chirp rate μ determine the features of chirp signal.

4.1. Reactivity estimation

The reactivity estimations for the chirp and step reactivity inputs are illustrated in [Figs. 1 and 2](#). The estimator parameters are selected as $\delta_r = 10$ for reactivity estimator (13), $\tau = 0.05$ for low pass filter (17) and $\varepsilon = 0.01$ for $\text{sat}(\cdot)$ function (26). In [Fig. 1a](#), the net reactivity estimation is given for the chirp reactivity input signal, $\rho_{in} = 0.008 \sin 2\pi t(0.01 + 0.4t)$. Since actual model and estimator have different initial conditions ($N_0 = 0.6$ and $\hat{N}_0 = 0.71$), the estimator converges to the actual reactivity at around 0.4 s. In [Fig. 1b](#), the input reactivity has a step change at the time $t = 50$ s and again it takes 0.4 s for estimator convergence to the actual reactivity. It is obvious from figures that the proposed reactivity estimator provides excellent reactivity estimation results.

[Fig. 2](#) shows reactivity estimation results for the chirp reactivity input signal under noisy neutron power measurement. While the noise on reactor power measurement is about $\pm 5\%$ of the normalized power value, the net reactivity is estimated perfectly. Small fluctuations on the estimated reactivity are due to noisy power measurement, but its effect is minimized by the second-order low pass filter. Under noisy power measurement, the time constant of the low pass filter τ must be selected carefully to minimize the effect of the noise on the estimated reactivity because the effect of measurement noise is becoming larger when reactivity is decreasing.

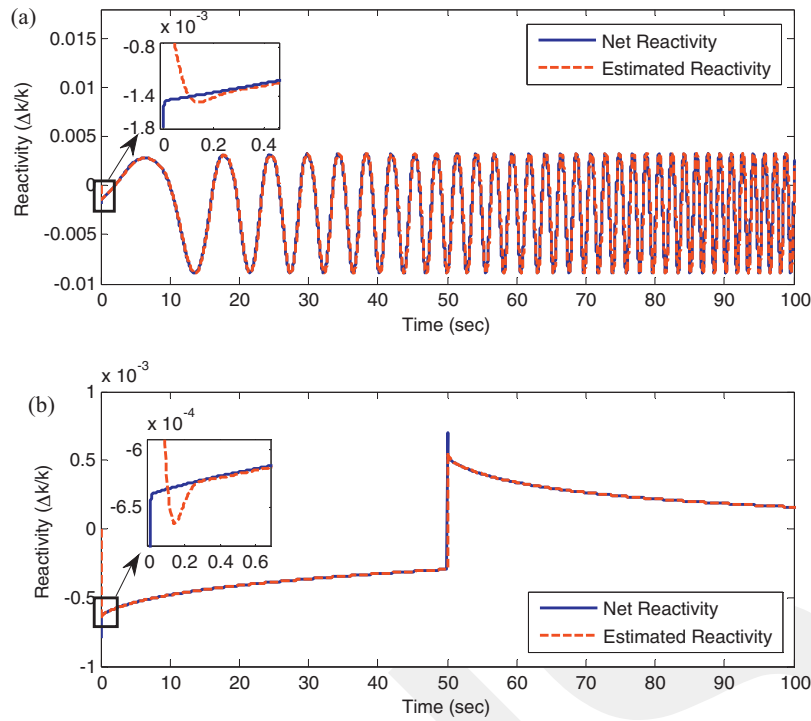


Fig. 1. Reactivity estimations for (a) chirp input reactivity and (b) step input reactivity excitations.

Fig. 3 displays reactivity estimation error for chirp input reactivity excitation under noisy neutron power measurement (compare with Fig. 2b). It is obvious that reactivity estimation error is very small for constant or slowly varying reactivities as seen in the first 10 s of Fig. 3, but becoming larger with increasing frequency of the reactivity. Hence, we can deduce that the slower reactivity input variations is, the smaller reactivity estimation error is obtained, and vice versa.

4.2. External neutron source estimation

The external neutron source estimation is illustrated in Fig. 4 for the step neutron inputs. The estimator parameters are selected as $\delta_s = 300$ for external neutron source estimator (18), $\tau = 0.2$ for low pass filter (21) and $\varepsilon = 0.01$ for $\text{sat}(\cdot)$ function (26). It is assumed that the reactivity input is a constant, $\rho_{\text{in}} = 8 \times 10^{-3} \Delta k/k$. Fig. 4a displays the external source estimation result for non-noisy power

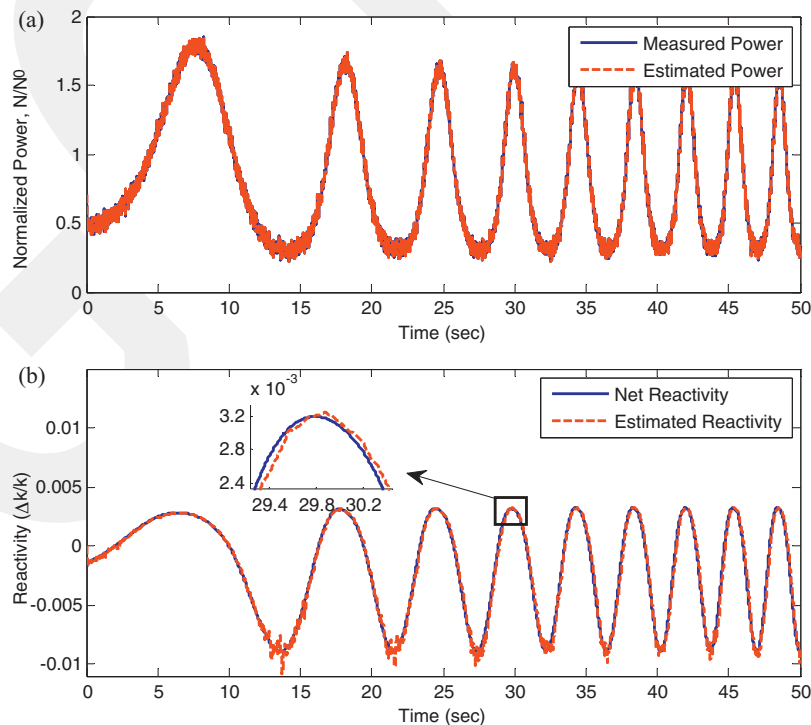


Fig. 2. Reactivity estimation under noisy neutron power measurement, (a) normalized neutron power and (b) chirp input reactivity excitations.

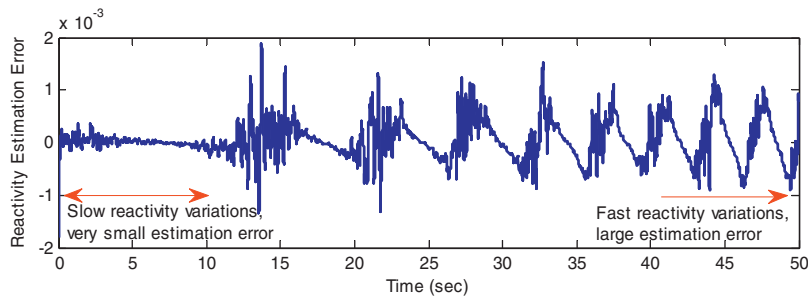


Fig. 3. Reactivity estimation error for chirp input reactivity excitations under noisy neutron power measurement.

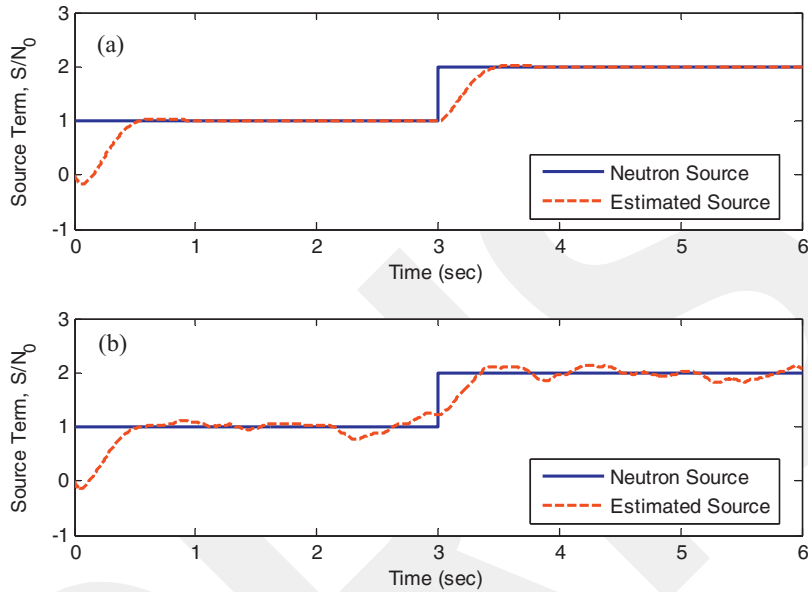


Fig. 4. Estimation of external neutron source normalized to power, (a) source estimation without noisy power measurement and (b) source estimation under noisy power measurement.

measurement, and Fig. 4b shows the same estimation when power measurement is polluted with noise. Since actual model and estimator have different initial conditions ($N_0 = 0.6$ and $\hat{N}_0 = 0.71$), the source estimator converges to the actual source at around 0.4 s. The small fluctuations on the estimated source are due to noisy power measurement, but again its effect is minimized by the second-order low pass filter. It is obvious from the figures that the proposed external source estimator provides excellent estimation results.

4.3. Precursor concentration estimation

The precursor estimation results are illustrated in Figs. 5–7. It is assumed that the reactivity input is a chirp signal for actual

system, but it is taken as constant for the precursor estimator as illustrated in Fig. 5. The estimator parameters are selected as $\delta_c = 300$ for precursor estimator (22), and $\varepsilon = 0.01$ for $\text{sat}(\cdot)$ function (26). Fig. 6 displays the precursor estimation result. Because actual model and estimator have different initial conditions ($N_0 = 0.6$ and $\hat{N}_0 = 0.71$), the estimated precursors converge to the actual precursors at around $4/\lambda_1 = 317$ s for \hat{C}_1 , $4/\lambda_2 = 132$ s for \hat{C}_2 , $4/\lambda_3 = 35.78$ s for \hat{C}_3 , $4/\lambda_4 = 13.27$ s for \hat{C}_4 , $4/\lambda_5 = 3.52$ s for \hat{C}_5 , and $4/\lambda_6 = 1.32$ s for \hat{C}_6 . Note that the settling time here is taken as $4/\lambda$ for a time constant λ (decay constant). The proposed precursor estimator provides excellent estimation results even though the actual PRK and precursor estimator have different initial conditions and reactivity input values.

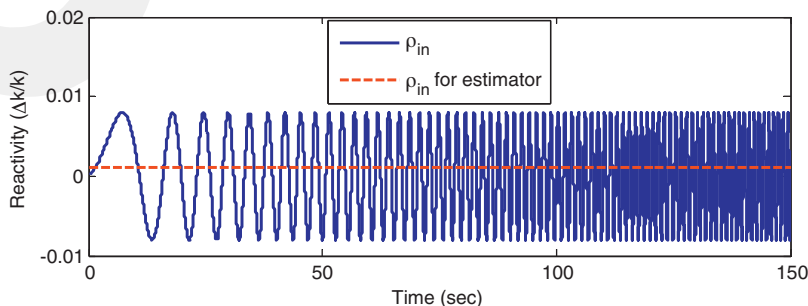


Fig. 5. External reactivity inputs, chirp signal for the PRK system and a constant signal for its estimator.

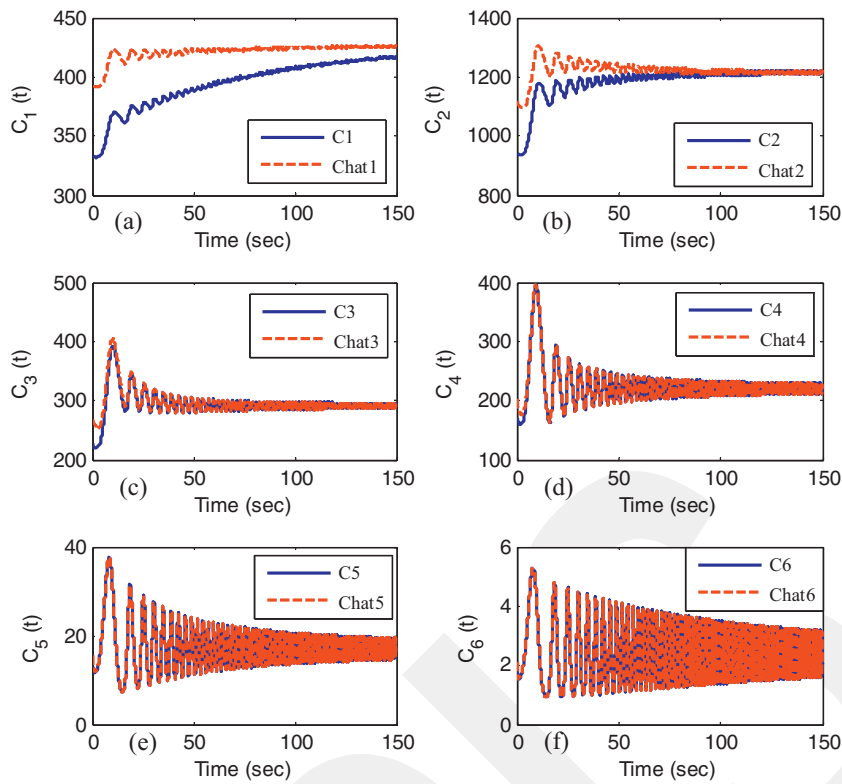


Fig. 6. Estimation of precursor concentrations normalized to N_0 , (a) C_1 and its estimation \hat{C}_1 , (b) C_2 and its estimation \hat{C}_2 , (c) C_3 and its estimation \hat{C}_3 , (d) C_4 and its estimation \hat{C}_4 , (e) C_5 and its estimation \hat{C}_5 , and (f) C_6 and its estimation \hat{C}_6 .

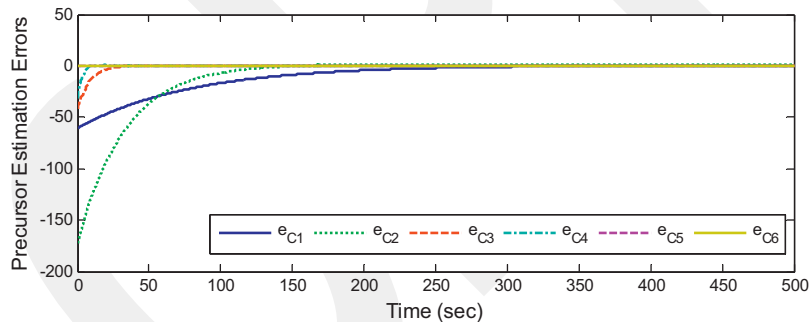


Fig. 7. Estimation errors for precursor concentrations.

Fig. 7 illustrates the precursor estimation errors. Similar to the explanations of Fig. 6, the estimation errors converge to zero with the settling time $4/\lambda_i$, e.g. $4/\lambda_1 = 317$ s for e_{C_1} , $4/\lambda_2 = 132$ s for e_{C_2} and so on. It should be noted that the larger the estimator gain δ_c is, the smaller precursor estimation errors can be obtained. The numerical results agree with the theoretical foundations given in Section 3.3.

5. Conclusion

The paper has investigated robust reactivity, external neutron source, and precursor estimation algorithms through dynamic-nonlinear estimators. The estimators are designed based on nonlinear reactor kinetics equations and nonlinear estimation theory for robust quantity estimations. The estimation algorithms remove disadvantages of linear estimation approaches including limited bandwidth and performance degradation during operation point variations. The results demonstrate that the estimation

approaches provide reliable and accurate reactivity, neutron source and precursor concentration calculations while there exist initial condition and parameter uncertainties, and noisy measurements, which will increase control flexibility and safety of nuclear reactors.

References

- Ablay, G., Aldemir, T., 2011. Observation of the dynamics of nuclear systems using sliding mode observers. *Nucl. Technol.* 174, 64–76.
- Ablay, G., Aldemir, T., 2013. Fault detection in nuclear systems using sliding mode observers. *Nucl. Sci. Eng.* 173, 82–98.
- Aboanber, A.E., 2006. Stability of generalized Runge–Kutta methods for stiff kinetics coupled differential equations. *J. Phys. A: Math. Gen.* 39, 1859–1876.
- Albuquerque, J.S., Biegler, L.T., 1996. Data reconciliation and gross-error detection for dynamic systems. *AIChE J.* 42, 2841–2856.
- Ansari, S.A., 1991. Development of on-line reactivity meter for nuclear reactors. *IEEE Trans. Nucl. Sci.* 38, 946–952.
- Cacuci, D.G. (Ed.), 2010. *Handbook of Nuclear Engineering*. Springer.
- Cadini, F., Zio, E., 2007. A Monte Carlo method for the model based estimation of nuclear reactor dynamics. *Ann. Nucl. Energy* 34, 773.
- Dong, Z., Feng, J., Huang, X., 2009. Nonlinear observer-based feedback dissipation load-following control for nuclear reactors. *IEEE Trans. Nucl. Sci.* 56, 272–285.

- Gallmeier, F., Steichele, E., 1994. Neutron flux and reactivity calculations for an optimized arrangement of experimental facilities in a research reactor. *Nucl. Eng. Des.* 147, 437–446.
- Grauf, E., Jansky, J., Langenstein, M., 2000. Reconciliation of process data in Nuclear Power Plants (NPPs). In: Presented at the International Conference on Nuclear Engineering, Baltimore, MD USA.
- Hashemian, H.M., Feltus, M.A., 2006. On-line condition monitoring applications in nuclear power plants. In: NPIC and HMIT, Albuquerque, NM, USA.
- Hetrick, D.L., 1993. *Dynamics of Nuclear Reactors*. American Nuclear Society.
- Hines, J.W., Davis, E., 2005. Lessons learned from the US nuclear power plant on-line monitoring. *Prog. Nucl. Energy* 46, 176.
- Hu, Y., Zhao, Y., Chen, X., Xu, L., 2013. Proposing of a new fitting and iteration method (FIM) to correct measured reactor core reactivity. *Nucl. Eng. Des.* 254, 33–42.
- Humberstone, M., Wood, B., Henkel, J., Hines, W., 2011. An adaptive model for expanded process monitoring. *Nucl. Technol.* 173, 35–45.
- Pázsit, I., Ceder, M., Kuang, Z., 2004. Theory and analysis of the Feynman-Alpha method for deterministically and randomly pulsed neutron sources. *Nucl. Sci. Eng.* 148, 67–78.
- Khalil, H.K., 2002. *Nonlinear Systems*, 3rd ed. Prentice Hall.
- Li, Q., Bernard, J.A., 2002. Design and evaluation of an observer for nuclear reactor fault detection. *IEEE Trans. Nucl. Sci.* 49, 1304.
- Lu, X.-Y., Hedrick, J.K., 2000. Integral filters from a new viewpoint and their application in nonlinear control design. In: Presented at the Proceedings of the 2000 IEEE International Conference on Control Applications, pp. 501–506.
- Marseguerra, M., Zio, E., Torri, G., 2003. Power density axial oscillations induced by xenon dynamics: parameter identification via genetic algorithms. *Prog. Nucl. Energy* 43, 365.
- Martin, R.P., Edwards, R.M., 2000. A best-estimate reactor core monitor using state feedback strategies to reduce uncertainties. *Nucl. Sci. Eng.* 134, 293–305.
- Mihalcz, J.T., Blakeman, E.D., Ragan, G.E., Johnson, E.B., Hachiya, Y., 1990. Dynamic subcriticality measurements using the ^{252}Cf -source-driven noise analysis method. *Nucl. Sci. Eng.* 104, 314–338.
- Muñoz-Cobo, J.-L., Berglöf, C., Peña, J., Villamarín, D., Bournos, V., 2011. Feynman- α and Rossi- α formulas with spatial and modal effects. *Ann. Nucl. Energy* 38, 590–600.
- Na, M.G., No, H.C., 1992. Design of an adaptive observer-based controller for the water level of steam generators. *Nucl. Eng. Des.* 135, 379–394.
- Nahla, A.A., 2010. Analytical solution to solve the point reactor kinetics equations. *Nucl. Eng. Des.* 240, 1622–1629.
- Neeb, K.-H., 1997. *The Radiochemistry of Nuclear Power Plants With Light Water Reactors*. Walter de Gruyter.
- Park, Y.H., Cho, N.Z., 1992. A compensator design controlling neutron flux distribution via observer theory. *Ann. Nucl. Energy* 19, 513–525.
- Perez-Cruz, J.H., Poznyak, A., 2007. Estimation of the precursor power and internal reactivity in a nuclear reactor by a neural observer. In: Fourth International Conference on Electrical and Electronics Engineering, ICEEE 2007, pp. 310–313.
- Qaiser, S., Bhatti, A., Iqbal, R., Samar, A., Qadir, J., 2009. Estimation of precursor concentration in a research reactor by using second order sliding mode observer. *Nucl. Eng. Des.* 239, 2134–2140.
- Rác, A., 1992. On the estimation of a small reactivity change in critical reactors by Kalman filtering technique. *Ann. Nucl. Energy* 19, 527–538.
- Rasmussen, B., Davis, E., Hines, J.W., 2002. Monte Carlo analysis and evaluation of the instrumentation and calibration monitoring program. In: Maintenance and Reliability Conference, Knoxville, TN.
- Reddy, G.D., Bandyopadhyay, B., Tiwari, A.P., Fernando, T., 2008. Spatial control of a large pressurized heavy water reactor using sliding mode observer and control. In: International Conference on Control, Automation, Robotics and Vision, Hanoi, Vietnam.
- Sathiyasheela, T., 2010. Inhomogeneous point kinetics equations and the source contribution. *Nucl. Eng. Des.* 240, 4083–4090.
- Shampine, L.F., Reichelt, M.W., 1997. The Matlab ODE suite. *SIAM J. Sci. Comput.* 18, 1–22.
- Shaver, M.W., Lanning, D.D., 2010. Secondary Startup Neutron Sources as a Source of Tritium in a Pressurized Water Reactor (PWR) Reactor Coolant System (RCS) (No. PNNL-19151). Pacific Northwest National Laboratory, Richland, WA.
- Shtessel, Y.B., 1998. Sliding mode control of the space nuclear reactor system. *IEEE Trans. Aerosp. Electron. Syst.* 34, 579.
- Theler, G.G., Bonetto, F.J., 2010. On the stability of the point reactor kinetics equations. *Nucl. Eng. Des.* 240, 1443–1449.
- Upadhyaya, B.R., Zhao, K., Xu, X., 2005. Autonomous control of space reactor systems. In: Annual Report prepared for the US Department of Energy NEER Program.
- Wang, P., Aldemir, T., Utkin, V.I., 2001. Estimation of xenon concentration and reactivity in nuclear reactors using sliding mode. In: IEEE Conference on Decision and Control, Orlando, FL, p. 1801.
- Wright, J., 2005. Development and Investigation of Reactivity Measurement Methods in Subcritical Cores. Chalmers University of Technology, Department of Reactor Physics, Göteborg, Sweden (PhD dissertation).
- You, C., Kim, I., Han, S., Jeong, J., Kim, D., 2012. Performance improvement of ranging and communication system using ultra wide-band tilted frequency chirp signal. In: Wu, Y. (Ed.), *Advances in Computer, Communication, Control and Automation*, Lecture Notes in Electrical Engineering. Springer Berlin Heidelberg, pp. 313–320.
- Zavaljevski, N., Miron, A., Yu, C., Wei, T., Davia, E., 2004. A study of on-line monitoring uncertainty based on Latin hypercube sampling and wavelet denoising. In: International Topical Meeting on Nuclear Plant Instrumentation, Ohio.